Proceedings of the 21st ICSMGE, Vienna, Austria, 14 – 19 June 2026. Pistrol, Adam & Schweiger (eds.)
Published by: ÖGG, Austrian Society for Geomechanics, Salzburg, Austria, ISBN 978-3-9503898-4-5
https://doi.org/10.53243/ICSMGE2026-405

Centrifuge Model Test of Seismic Response of an Immersed Tunnel on Liquefiable Sand Deposit Under Horizontal Excitation

Huanzhu Zhou, Shengan Liu, Junjie Zheng, Yewei Zheng
School of Civil Engineering, Wuhan University, China, huanzhuz@whu.edu.cn

ABSTRACT: In coastal areas, immersed tunnels have been successfully used around the world owing to the advantages of strong adaptability to complex hydrogeological environments and high structural stability. The immersed tunnels may have to be constructed on liquefiable sand deposit, posing a potential threat to the safe operation of immersed tunnels when subjected to earthquake excitations. A centrifuge shaking table test was carried out to investigate the seismic response of an immersed tunnel on liquefiable sand under horizontal excitation. The centrifuge model for the immersed tunnel on liquefiable sand was designed according to the similitude relationships. The liquefiable sand was deposited using fine sand at a low relative density of 45%, and the backfill layer around the immersed tunnel was constructed using coarse sand with a higher relative density of 85%. Results indicated that the middle layer of liquefiable sand is the most susceptible to full liquefaction during horizontal excitation. The generation rate of excess pore water pressure gradually decreases from the middle to the upper layer. The softening and damping effects induced by sand liquefaction obstruct shear wave transmission upward. In the liquefiable sand deposit, the horizontal accelerations decrease with decreasing depth. The amplitudes of horizontal accelerations increase from the base to the top along the middle wall of the immersed tunnel due to the amplification effect with increasing elevation for the stiff tunnel structure. The uplift of the immersed tunnel lags behind the accumulation of excess pore water pressure in the underlying liquefiable sand.

KEYWORDS: Immersed tunnel, liquefaction, seismic response, centrifuge test, horizontal excitation.

1 INTRODUCTION

In coastal engineering, immersed tunnels have been successfully adopted worldwide due to their strong adaptability to complex hydrogeological conditions and high structural stability (Hu et al., 2015; Tsinidis et al., 2020; Zhou et al., 2024). However, extensive liquefiable sand deposits are often found in these areas. Sand liquefaction during earthquakes may cause uplift of tunnel, resulting in severe damage to the tunnel structure (Miranda et al., 2020; Jiang et al., 2024; Li et al., 2025). Significant ground motions and displacements were observed in the undersea Senkai Tunnel during the 1993 Hokkaido Southwestern Offshore earthquake and in the Marmaray immersed tunnel during the 2014 North Aegean earthquake due to sand liquefaction (Ikuma, 2005; Dikmen, 2016). Therefore, understanding the seismic response of immersed tunnels on liquefiable sand is of critical importance. These cases highlight the urgent need to better understand the behavior of immersed tunnels on liquefiable sand deposits under earthquake excitations.

Previous investigations have largely concentrated on the seismic behavior of shield tunnels embedded in liquefiable soils (Shen et al., 2022; Wu et al., 2023; Yao et al., 2023; Wu et al., 2024; Shen et al., 2025; Xu et al., 2025). These studies have identified various failure mechanisms during strong ground motion, such as tunnel uplift, racking deformation, and pronounced internal forces acting on the lining system (Shen et al., 2024). The uplift of tunnel, may cause serious structural damage, including segment separation, water ingress, and voids between the tunnel and surrounding ground. This uplift is primarily driven by the upward seepage flow generated by excess pore water pressure, which causes water and soil particles to migrate toward the tunnel crown. As such, the surrounding soil is displaced and squeezes into the arch bottom, leading to the uplift of shield tunnel (Chen et al., 2023). The shield tunnels move with the surrounding soils during earthquake due to the strong constraints at large burial depth. In contrast, immersed tunnels are generally buried at shallower depths, often with only 2-4 m thick overlying backfill, which provides much less restraint. Consequently, immersed tunnels are more vulnerable to large deformations during seismic shaking. Understanding their response under such conditions is therefore essential.

In this study, centrifuge shaking table test was conducted to investigate the seismic response of an immersed tunnel on liquefiable sand under horizontal excitation. The experiments captured excess pore water pressure in the liquefiable sand deposit, acceleration responses, and uplift displacement of the immersed tunnel.

2 CENTRIFUGE MODEL TEST

2.1 *Centrifuge test apparatus and scaling law*

The tests were conducted using the TK-C500 geotechnical centrifuge and an electro-hydraulic shaking table at the Tianjin Research Institute for Water Transport Engineering. Under a centrifugal acceleration of 100 g, the system achieves a maximum horizontal input acceleration of 0.4 g. To minimize dynamic boundary effects induced by horizontal shaking, a flexible laminar container was employed. This container, with internal dimensions of 800 mm in length, 350 mm in width, and 600 mm in height, was lined with a 2 mm thick latex membrane to prevent fluid leakage. In this study, the material properties, geometry, and earthquake motion were scaled using the similitude laws recommended by Schofield (1981). A geometric scale factor of 1:100 was adopted to accommodate the available space in the container. The corresponding scaling parameters are detailed in Table 1.

Table 1. Similitude laws of the centrifuge shaking table tests (Schofield, 1981).

Physical quantity	Model	Prototype (N=100)
Displacement	1	100
Time (diffusion)	1	100^2
Time (dynamic)	1	100
Frequency	1	100
Acceleration	1	100
Flexural stiffness	1	100^4
Velocity	1	1
Stress	1	1

As illustrated in Table 1, when water is used as the pore fluid in centrifuge tests, a conflict arises between the time scaling factors of the diffusion process and the dynamic process. To resolve the conflict of time scaling between the diffusion process (scaling as 100^2) and the dynamic loading (scaling as 100), silicone oil with a density of 970 kg/m³ and 100 times the viscosity of water was used. The silicone oil could mimic the properties of water while increasing its viscosity, ensuring that both processes could be scaled as 100.

2.2 *Model dimensions*

Figure 1 presents a schematic view of the centrifuge model used to simulate an immersed tunnel on liquefiable sand. The centrifuge model represents a level site with a depth of 55 m. From bottom to top, the model comprises liquefiable sand layer, gravel bed, immersed tunnel, backfill layer, and overlying fluid. The liquefiable sand and gravel bed have thicknesses of 32.4 m and 1.4 m, respectively. The vertical distance from the tunnel base to the fluid surface is 10.1 m, while the backfill above the tunnel measures 2.1 m. The fluid extends to a depth of 12.5 m.

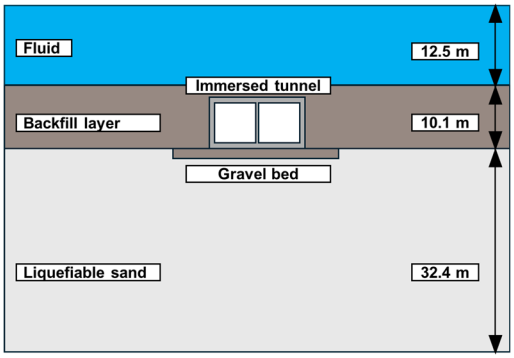

Figure 1. Schematic view of the immersed tunnel in liquefiable sand (dimensions in prototype scale).

2.3 *Preparation and saturation of sands*

In this study, the model was constructed using the dry pluviation method where the relative density was controlled by the weight of sand for each lift falling from a specific height. Fujian fine sand with particle sizes below 0.5 mm was used to simulate the liquefiable sand layer. During air pluviation, a 32.4 m-thick layer of dry Fujian fine sand was deposited to form the liquefiable stratum, achieving a low relative density of D_r = 45%, representative of loose sand conditions commonly used in liquefaction studies. The dry fine sand had a density of 1.486 g/cm³. Fujian coarse sand (1-2 mm) was adopted for both the gravel bed and backfill layer in immersed tunnel projects (Xu et al., 2018). For the 1.4 m-thick gravel bed and the 10.1 m-thick backfill layer, a dense layer of Fujian coarse sand was dry pluviated to model the compacted block and crushed stones with particle size of 60-200 mm typically used in field applications (Xu et al., 2018). The coarse sand had a relative density of D_r = 85% and a density of 1.658 g/cm³. The properties of the Fujian fine sand and coarse sand used in the centrifuge shaking table test are presented in Table 1.

Table 1. Properties of Fujian sand.

Property	Fine sand	Coarse sand
Maximum void ratio, e_{max}	1.0	0.9
Minimum void ratio, e_{min}	0.6	0.5
Maximum dry density, $\rho_{d\,max}$ (g/cm^3)	1.6	1.7
Minimum dry density, $\rho_{d\,min}$ (g/cm^3)	1.3	1.4
Maximum particle size, d_{max} (mm)	0.5	2.0

2.4 *Instrumentation*

Five pore water pressure sensors (PWP sensors), five horizontal accelerometers and a linear variable displacement transducer (LVDT) were instrumented for the model, as shown in Figure 2. Sensors PP1 to PP5 and A1 to A5 were positioned 38.1 m from the left boundary of the flexible laminar container and 1.9 m offset from the tunnel's centerline. Among them, three PWP sensors (PP1, PP2, and PP3) and three accelerometers (A1, A2, and A3) were installed within the liquefiable sand at the depths of d = 39.0 m, 33.0 m, and 25.0 m below the fluid surface level (d = 0 m). PP4 was placed within the gravel bed at the depth of 23.0 m, while PP5 was placed in the backfill layer at 13.5 m, representing positions beneath and above the tunnel, respectively. Two accelerometers A4 and A5 were placed at the base and top of the middle wall of the immersed tunnel, respectively. An LVDT was mounted vertically at the central position on the roof slab of the immersed tunnel, at a depth of d = 14.5 m, to monitor its vertical displacement.

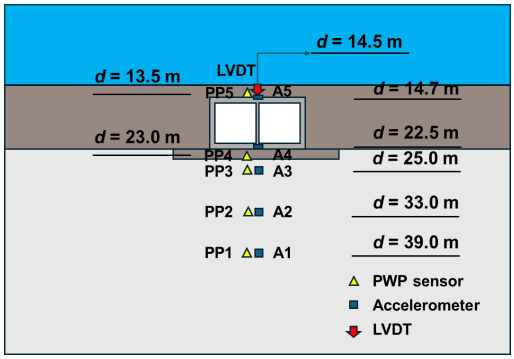

Figure 2. Centrifuge model configuration.

2.5 *Testing procedures and input motions*

The centrifuge was ramped up to 100g in 10g increments, with a spin-up rate of 0.09 g/s at each stage. At each g-level, sufficient time was maintained to allow pore water pressure and surface settlement to stabilize.

In this study, seismic input motions were derived from a marine earthquake that occurred in Japan in 2013 (magnitude ML = 6.4), based on records from the K-NET database maintained by the National Research Institute for Earth Science and Disaster Resilience (NIED). The selected ground motion was recorded at station KNG202 (139.8393°E, 34.7396°N), located on the seabed off the coast of Japan. The input excitation features dominant frequencies between 1 Hz and 2 Hz. After filtering, baseline correction, and amplitude scaling, the horizontal acceleration time histories used in the centrifuge shaking table tests are presented in Figure 3, with a peak acceleration of 0.1g.

Figure 3. Time histories of input horizontal excitations.

3 TEST RESULTS

The seismic response of an immersed tunnel on liquefiable sand was analyzed based on the excess pore water pressures and accelerations in the liquefiable sand, and accelerations and uplift displacements of the immersed tunnel. This analysis aims to provide insights into the seismic response of an immersed

tunnel on liquefiable sand subjected to horizontal excitation. Throughout the remainder of this paper, all units are presented in prototype scale, unless specified otherwise.

3.1 *Excess pore water pressures*

Figure 4 shows the time histories of excess pore water pressure, u_e, at different depths near the centerline of the model under horizontal excitation. The dashed lines represent the initial effective overburden stresses at the corresponding depths. When the excess pore water pressure exceeds the initial effective overburden stress, it indicates full liquefaction at that depth.

In the liquefiable sand, the excess pore water pressure initially exhibits slight fluctuations around zero, then increases rapidly before reaching stable. The maximum excess pore water pressure exceeds initial effective overburden stress at the depth of 39.0 m; however, the maximum excess pore water pressures do not exceed the initial effective overburden stresses at the depths of 33.0 m and 25.0 m, indicating that full liquefaction of the sand occurs only around the depth of 39.0 m. The generation rate of excess pore water pressure refers to the speed of the excess pore water pressure increasing from nearly zero to the stabilized value. From the middle layer to the upper layer (from d = 39 m to d = 33 m to d = 25 m), the generation rate of excess pore water pressure in the liquefiable sand gradually decreases. This is because the upper part of the liquefiable sand is close to the gravel bed and backfill layer with higher permeability. The stronger drainage capacity of these layers makes it less likely for excess pore water pressure to accumulate in the upper part of the liquefiable sand. In the gravel bed and backfill layer beneath and above the immersed tunnel (at d = 23 m and d = 13.5 m), respectively, the excess pore water pressure shows only a slight increase and almost no change, respectively, and the maximum excess pore water pressure is significantly smaller than the initial effective overburden stress. This is because the high permeability and strong drainage capacity of the gravel bed and backfill layer effectively hinder the accumulation of excess pore water pressure.

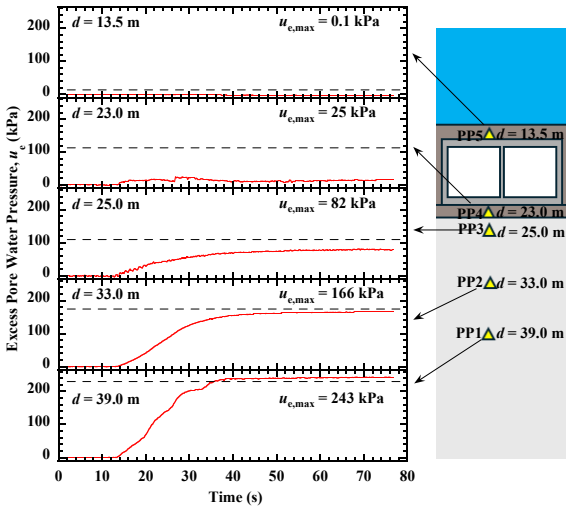

Figure 4. Time histories of excess pore water pressure in the vertical direction during horizontal excitation.

3.2 *Horizontal accelerations*

Figure 5 shows the time histories of horizontal accelerations along the vertical direction under earthquake excitation. Horizontal accelerations within the liquefiable sand layer are illustrated by the curves between the depths of 39.0 m and 25.0 m. The depths of 22.5 m and 14.7 m correspond to the base and top of the middle wall of the immersed tunnel, respectively. The time history of horizontal accelerations at the depth of 39.0 m where full liquefaction occurred exhibit distinct characteristics during earthquake excitation. Initially, the horizontal accelerations are relatively small, fluctuating slightly around zero. Subsequently, the amplitude of these fluctuations increases rapidly, peaking during the main shocking event, which lasts from 12 s to 38 s. After this period, the horizontal acceleration decreases abruptly and remains at a relatively low value before eventually returning to zero. This is because the excess pore water pressure at the depth of 39.0 m does not exceed the initial effective overburden stress before 38 s but exceeds the initial effective overburden stress after 38 s. This indicates that full liquefaction does not occur at the depth of 39.0 m before 38 s but occurs after 38 s. Therefore, the horizontal accelerations at the depth of 39.0 m show amplification before 38 s. After 38 s, in addition to the attenuation of input earthquake excitations, the softening and damping effects induced by full liquefaction of sand also contribute to the decrease in horizontal accelerations over time. As shown in Figure 5, as the depth of the liquefiable sand decreases to d = 33.0 m and 25.0 m, the amplitudes and duration of relatively high-amplitude fluctuations become significantly shorter, which indicates that the softening and damping effects induced by sand liquefaction could obstruct the shear wave transmission over the depth upward.

Figure 5 illustrates that, with a further decrease in depth, the horizontal accelerations at the base of the middle wall of the immersed tunnel are slightly smaller than those observed at d = 25 m due to the attenuation effect of gravel bed. The amplitudes of horizontal accelerations increase from the base to the top along the middle wall of the immersed tunnel, which is attributed to the amplification effect of horizontal accelerations with increasing elevation for the stiff tunnel structure.

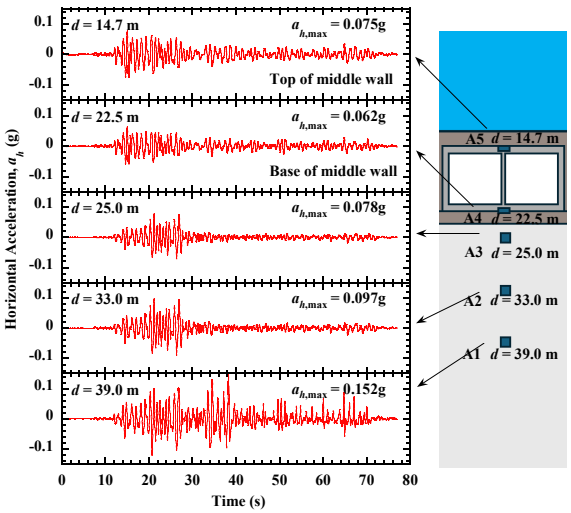

Figure 5. Time histories of horizontal accelerations in the vertical direction during horizontal excitation.

3.3 *Uplift displacements*

Figure 6 presents the time histories of the vertical displacement of the immersed tunnel during horizontal excitation. The development of vertical displacements during horizontal excitation can be divided into three stages. During the initial phase (Stage 1), the displacement remains nearly stable, fluctuating slightly around zero. In Stage 2, the tunnel begins to subside, reaching the maximum downward displacement. This sinking phase occurs approximately between 12.0 s and 22.0 s, coinciding with the onset of excess pore water pressure accumulation at around 12.0 s. In the subsequent Stage 3, which

represents the upward movement of the immersed tunnel, the displacement transitions from the lowest point to the peak in the upward direction, lasting from approximately 22.0 s to 77.0 s. This suggests that, during earthquake excitation, the uplift of the immersed tunnel lags behind the build-up of excess pore water pressure in the underlying liquefiable sand. Figure 6 shows that the immersed tunnel exhibits a significant residual upward displacement of 229 mm. This magnitude of uplift displacement may cause damage to the tunnel structure.

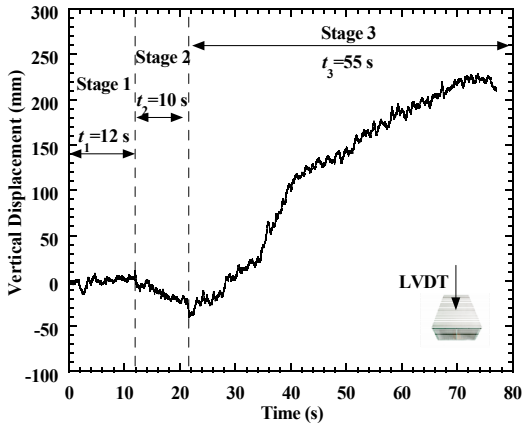

Figure 6. Time histories of vertical displacement of the immersed tunnel during horizontal excitation.

4 CONCLUSIONS

A centrifuge shaking table test was performed to study the seismic response of an immersed tunnel on liquefiable sand under horizontal excitation. Detailed information on the experimental similitude design, model setup, measurement instrumentation, and earthquake motion were provided. Test results provide valuable references for future research. The key findings of this study are summarized below:

(1) The generation of excess pore water pressure in liquefiable sand exhibits an initial stable phase, followed by an increase and subsequent stabilization during earthquake excitation. The middle layer of liquefiable sand is the most susceptible to full liquefaction during horizontal excitation. The rate of excess pore water pressure generation gradually decreases from the middle to the upper layer due to the high permeability and strong drainage capacity of the gravel bed and backfill.

(2) The softening and damping effects induced by sand liquefaction cause abrupt attenuation of horizontal accelerations after the occurrence of full liquefaction. The horizontal accelerations decrease with decreasing depth in the liquefiable sand, as liquefaction obstructs shear wave transmission upward. The amplitudes of horizontal accelerations increase from the base to the top along the middle wall of the immersed tunnel due to the amplification effect with increasing elevation for the stiff tunnel structure.

(3) The vertical displacement of the immersed tunnel exhibits an initial stable phase, followed by downward subsidence and subsequent upward movement. The uplift of the immersed tunnel lags behind the accumulation of excess pore water pressure in the underlying liquefiable sand and could cause significant damage to the tunnel structure.

5 ACKNOWLEDGEMENTS

This research is supported by the National Key R&D Program of China (Grant No. 2022YFC3080400) and the National Natural Science Foundation of China (Grant No. 52078236, 52078392, 52338007, and 52478358). The authors gratefully acknowledge the financial supports.

6 REFERENCES

Chen, X.S., Shen, J., Bao, X.H., Wu, X.L., Tang, W.C., and Cui, H.Z. 2023. A review of seismic resilience of shield tunnels. *Tunnelling and Underground Space Technology* 136, 105075.

Dikmen, S.U. 2016. Response of Marmaray Submerged Tunnel during 2014 Northern Aegean Earthquake (Mw=6.9). *Soil Dynamics and Earthquake Engineering* 90, 15-31.

Hu, Z.N., Xie, Y.L., and Wang, J. 2015. Challenges and strategies involved in designing and constructing a 6 km immersed tunnel: A case study of the Hong Kong-Zhuhai-Macao Bridge. *Tunnelling and Underground Space Technology* 50, 171-177.

Ikuma, M. 2005. Maintenance of the undersea section of the Seikan Tunnel. *Tunnelling and Underground Space Technology* 20 (2), 143-149.

Jiang, J.W., Xun, Z., Bai, X.X., Liu, D., Zhao, K., and Du, X.L. 2024. Seismic damage mechanics and vulnerability analysis for the immersed tunnel subjected transverse earthquake records. *Soil Dynamics and Earthquake Engineering* 182, 108703.

Li, Y., Wang, R., Ma, H.B., and Zhang, J.M. 2025. Rising groundwater table due to restoration projects amplifies earthquake induced liquefaction risk in Beijing. *Nature Communications* 16(1), 1466.

Miranda, L., Caldeira, L., Serra, J., and Gomes, R.C. 2020. Dynamic behaviour of Tagus River sand including liquefaction. *Bulletin of Earthquake Engineering* 18(10), 4581-4604.

Schofield, A.N. 1981. Dynamic and earthquake geotechnical centrifuge modeling, *Proc. International Conference on Recent Advances in Geotechnical Earthquake Engineering and Soil Dynamics*, Rolla, 1081-1100.

Shen, Y.Y., Zhong, Z.L., Li, L.Y., Du, X.L., and El Naggar, M.H. 2022. Seismic response of shield tunnel structure embedded in soil deposit with liquefiable interlayer. *Computers and Geotechnics* 152, 105015.

Shen, Y.Y., El Naggar, M.H., Zhang, D.M., Li, L., and Du, X.L. 2024. Seismic response characteristics of shield tunnel structures in liquefiable soils. *Soil Dynamics and Earthquake Engineering* 182, 108701.

Shen, J., Bao, X.H., Li, J.H., Chen, X.S., and Cui, H.Z. 2025. Study on the mechanism of EPWP dissipation at the joints of shield tunnel in liquefiable strata during seismic events. *Soil Dynamics and Earthquake Engineering* 188, 109089.

Tsinidis, G., De Silva, F., Anastasopoulos, I., Bilotta, E., Bobet, A., Hashash, Y.M.A., He, C., Kampas, G., Knappett, J., Madabhushi, G., Nikitas, N., Pitilakis, K., Silvestri, F., Viggiani, G., and Fuentes, R. 2020. Seismic behaviour of tunnels: From experiments to analysis. *Tunnelling and Underground Space Technology* 99, 103334.

Wu, H., Ye, Z., Zhang, Y.T., and Liu, H.B. 2023. Numerical study on seismic behavior of shield tunnel crossing saturated sandy strata with different densities. *Rock and Soil Mechanics* 44(4), 1204-1216.

Wu, H., Liu, H.B., Dai, Q.Q, An, X.Y., Zhang, Y.T., and Ye, Z. 2024. Centrifuge modeling of seismic loading on a tunnel crossing saturated sand deposits with different relative densities. *Soil Dynamics and Earthquake Engineering* 184, 108850.

Xu, G.P., Yuan, Y., and Su, Q.K. 2018. *Key Technology and Creation for Seismic Resistance of Immersed Tunnels* Beijing: China Communications Press Co., Ltd.

Xu, L.Y., Xi, J.P., Jiang, J.W., Cai, F., Sun, Y.J., and Chen, G.X. 2025. Seismic fragility analysis of shield tunnels in liquefiable layered deposits. *Soil Dynamics and Earthquake Engineering* 191, 109246.

Yao, A.J., Tian, T., Gong, Y.F., and Li, H. 2023. Shaking table tests of seismic response of multi-segment utility tunnels in a layered liquefiable site. *Sustainability* 15(7), 15076030.

Zhou, H.Z., Liu, S.A., Li, B., Chen, W.Y., Su, L., Zheng, J.J., and Zheng, Y.W. 2024. Comparative Analysis of Longitudinal Seismic Responses of Rigid, Flexible, and Semirigid Immersed Tunnels Using the Analytical Method. *International Journal of Geomechanics* 24 (12), 04024284.